JOURNAL OF MARINE RESEARCH

The *Journal of Marine Research,* one of the oldest journals in American marine science, published important peer-reviewed original research on a broad array of topics in physical, biological, and chemical oceanography vital to the academic oceanographic community in the long and rich tradition of the Sears Foundation for Marine Research at Yale University.

An archive of all issues from 1937 to 2021 (Volume 1–79) are available through EliScholar, a digital platform for scholarly publishing provided by Yale University Library at https://elischolar.library.yale.edu/.

Requests for permission to clear rights for use of this content should be directed to the authors, their estates, or other representatives. The *Journal of Marine Research* has no contact information beyond the affiliations listed in the published articles. We ask that you provide attribution to the *Journal of Marine Research.*

Yale University provides access to these materials for educational and research purposes only. Copyright or other proprietary rights to content contained in this document may be held by individuals or entities other than, or in addition to, Yale University. You are solely responsible for determining the ownership of the copyright, and for obtaining permission for your intended use. Yale University makes no warranty that your distribution, reproduction, or other use of these materials will not infringe the rights of third parties.

Nonlinear limits to ocean thermal structure

by N. P. Fofonoff[1]

ABSTRACT

The nonlinear volume changes associated with diffusion and mixing of different seawater types produce significant conversions of gravitational potential energy to kinetic energy to maintain and enhance mixing processes and to limit the magnitudes of temperature gradients that can persist in the ocean. Several examples are given to illustrate these critical temperature gradients beyond which conversion exceeds local energy consumption by mixing.

The vertical temperature gradients in the Gulf Stream reduce downstream from Cape Hatteras to the critical limit found in the North Atlantic thermocline. The limiting gradients are also seen in surface thermoclines and in ''staircase'' structures. Although the theoretical interpretation of the nonlinear limiting processes is still incomplete, the observational evidence is compelling for further study of these mechanisms.

1. Introduction

The change of volume that occurs when two masses of seawater of different temperatures and salinities are mixed together has several dynamical effects on the distribution of ocean properties. The change is usually a reduction of volume because of the increase of the thermal expansion coefficient with temperature. The volume decrease of the warmer water exceeds in magnitude the volume increase of the colder water. If the initial densities are the same because of salinity differences, the mixtures are of higher density and can result in a gravitational instability. This effect, usually called ''cabbeling,'' has been examined by many authors starting with Witte (1902) (Fofonoff, 1961; 1995).

The change of volume also occurs because of the dependence of compressibility on temperature. Cold water is more compressible than warm water. An increase of pressure on a column of water can also result in a gravitational instability, for example, for a convergent cold layer overlying warmer water. This type of convectional instability has been described by Gill (1973). A similar instability in the atmosphere caused by a change in pressure and release of latent heat by condensation is referred to as a Conditional Instability of the Second Kind (*CISK*), (Charney and Eliassen, 1964).

Another effect, discussed by Eckel (1949) and addressed in the present paper, is the change of Gravitational Potential Energy (*GPE*) accompanying the displacement by mixing of seawater masses relative to the geopotential field. A change in volume of a

---

1. Woods Hole Oceanographic Institution, Woods Hole, Massachusett, 02543, U.S.A.

seawater element has an external or global effect as well as a local effect because the volume change shifts mass relative to the geopotential field. This shift contributes to available potential energy and can exceed the local energy required for the displacement. The possibility of an instability and enhanced mixing exists that needs to be evaluated.

The changes of *GPE* are examined by evaluating the total change of *GPE* for two extreme cases. First, a mass element in a column of seawater is isolated from its surroundings and allowed to proceed by molecular diffusion toward equilibrium. The second consists of an isentropic exchange of mass elements followed by mixing by diffusion with surrounding seawater. This case is considered a simulation of active turbulent mixing. In both cases, if the total change of *GPE* is negative, i.e. the global decrease in *GPE* exceeds in magnitude the local increase, conversion of *GPE* to kinetic energy is possible and can result in accelerated or sustained mixing locally. The reduction in volume by mixing contributes to a downstream slope of pressure surfaces which become ''slippery'' when the decrease of global *GPE* of the overlying mass exceeds in magnitude the local increase and energy dissipation.

The magnitude of the volume change depends primarily on the vertical temperature gradient, although horizontal gradients can also contribute. A critical temperature gradient is reached when the external changes of *GPE* are equal and opposite to the local changes. Gradients larger in magnitude than the critical value will yield a net decrease of *GPE* and are assumed to be associated with higher mixing rates and structures with shorter time scales. Critical temperature gradients are reached at lower magnitudes than the diffusive gradients for the mixing case if the salinity gradient is destabilizing. Temperature gradients exceeding critical magnitudes are assumed to be indicative of regions of active mixing.

A number of examples are presented for which these two cases appear to limit the vertical temperature-salinity structure of the water column and may represent criteria for identifying active mixing regions of the ocean.

2. Isenthalpic perturbations by diffusion

If a portion of a seawater column is insulated from its surroundings and allowed to proceed toward equilibrium by molecular diffusion, the difference between the final and initial volumes, $\Delta V = V^f - V^i$, can be estimated as follows:

Let m represent a mass variable over a column segment from z_1 to z_2 of total mass M:

$$m = \int_{z_1}^{z} \rho\, dz, \qquad M = \int_{z_1}^{z_2} \rho\, dz,$$

where z is the vertical coordinate. The local change of *GPE*, $\Delta\chi_{local}$, is given by:

$$\Delta\chi_{local} = \int_{0}^{M} [\phi^f(m) - \phi^i(m)]\, dm = \int_{0}^{M} \Delta\phi(m)\, dm,$$

where ϕ^i, ϕ^f are the initial and final values of geopotential, $\phi(m) = \phi_0 + \int_{0}^{m} g\alpha(m)\, dm$, where ϕ_0 is the geopotential at the bottom of the mass segment, g is gravity and $\alpha(m)$,

specific volume, a function of pressure p, temperature t and salinity s. The global change of *GPE,* because of the change of volume of the segment, is given by:

$$\Delta \chi_{global} = p(M)\Delta V = p(M) \int_0^M \Delta\alpha(m) \, dm.$$

The total change of *GPE* is, therefore,

$$\Delta \chi_{global} + \Delta \chi_{local} = p(M) \int_0^M \Delta\alpha(m) \, dm + \int_0^M \Delta\phi(m) \, dm = \int_0^M \Delta p\alpha(m) \, dm. \quad (1)$$

The change of any thermodynamic function $\lambda(p, t, s)$ from initial to final states, $\Delta\Lambda = \int_0^M (\lambda^f - \lambda^i) \, dm$, can be estimated by expanding the function as a Taylor series in m and integrating over the column segment:

$$\Delta\Lambda = \int_0^M \Delta\lambda \, dm = \Delta\lambda_0 M + \frac{1}{2} \Delta \frac{d\lambda}{dm} M^2 + \frac{1}{6} \Delta \frac{d^2\lambda}{dm^2} M^3 + \cdots$$

Expanding $\Delta\Lambda$ in terms of pressure $p = p_0 - gm$, enthalpy h, and salinity s yields:

$$\Delta\Lambda = \frac{\partial\lambda}{\partial p}\left[\Delta p_0 M + \frac{1}{2}\Delta\frac{dp}{dm}M^2 + \frac{1}{6}\Delta\frac{d^2p}{dm^2}M^3 + \cdots\right]$$

$$+ \frac{\partial\lambda}{\partial h}\left[\Delta h_0 M + \frac{1}{2}\Delta\frac{dh}{dm}M^2 + \frac{1}{6}\Delta\frac{d^2h}{dm^2}M^3 + \cdots\right]$$

$$+ \frac{\partial\lambda}{\partial s}\left[\Delta s_0 M + \frac{1}{2}\Delta\frac{ds}{dm}M^2 + \frac{1}{6}\Delta\frac{d^2s}{dm^2}M^3 + \cdots\right]$$

$$+ \frac{1}{6}M^3\left[\frac{d}{dm}\left(\frac{\partial\lambda}{\partial p}\right)\Delta\frac{dp}{dm} + \frac{d}{dm}\left(\frac{\partial\lambda}{\partial h}\right)\Delta\frac{dh}{dm} + \frac{d}{dm}\left(\frac{\partial\lambda}{\partial s}\right)\Delta\frac{ds}{dm}\right] + \cdots$$

As no heat or mass is exchanged with the surroundings, the total mass M, enthalpy H, and salt content S of the column segment are conserved, i.e.,

$$\Delta M = \Delta \int_0^M dm = 0, \qquad \Delta p = g\Delta M = 0$$

$$\Delta H = \int_0^M \Delta h \, dm = \Delta h_0 M + \frac{1}{2}\Delta\frac{dh}{dm}M^2 + \frac{1}{6}\Delta\frac{d^2h}{dm^2}M^3 + \cdots = 0$$

$$\Delta S = \int_0^M \Delta s \, dm = \Delta s_0 M + \frac{1}{2}\Delta\frac{ds}{dm}M^2 + \frac{1}{6}\Delta\frac{d^2s}{dm^2}M^3 + \cdots = 0.$$

Applying the conservation equations, the change $\Delta\Lambda$ reduces to:

$$\Delta\Lambda = \frac{1}{6}M^3\left[+\frac{d}{dm}\left(\frac{\partial\lambda}{\partial h}\right)\Delta\frac{dh}{dm} + \frac{d}{dm}\left(\frac{\partial\lambda}{\partial s}\right)\Delta\frac{ds}{dm}\right] + \cdots \quad (2)$$

The total change of *GPE* is given by substituting $\lambda = p\alpha(m)$:

$$\Delta\chi_{total} = \frac{M^3}{6}\left[\frac{d}{dm}\left(p\frac{\partial\alpha}{\partial h}\right)\Delta\frac{dh}{dm} + \frac{d}{dm}\left(p\frac{\partial\alpha}{\partial s}\right)\Delta\frac{ds}{dm}\right] + \cdots$$

The enthalpy gradient can be replaced with the temperature and salinity gradients:

$$\Delta\frac{dh}{dm} = C_p\Delta\frac{dt}{dm} + C_s\Delta\frac{ds}{dm} \simeq C_p\Delta\frac{dt}{dm},$$

since $C_s = (\partial h/\partial s)_{p,t}$ is small (Feistel and Hagen, 1995). The total change of *GPE* can be approximated by:

$$\Delta\chi_{total} \simeq \frac{M^3}{6}\left[\frac{d}{dm}\left(p\frac{\partial\alpha}{\partial t}\right)\Delta\frac{dt}{dm} + \frac{d}{dm}\left(p\frac{\partial\alpha}{\partial s}\right)\Delta\frac{ds}{dm}\right], \tag{3}$$

neglecting variations of specific heat C_p.

Assuming that the temperature and salinity gradients are perturbed by diffusion, the changes within the segment by the vertical fluxes of heat and salt are approximated by:

$$F_q = -\rho C_p k_t\frac{dt}{dz} = -\rho^2 C_p k_t\frac{dt}{dm}$$

$$F_s = -\rho^2 k_s\left[\frac{ds}{dm} - \left(\frac{ds}{dm}\right)_{equil}\right],$$

where k_t, k_s are molecular diffusion coefficients for heat and salt.

As salt diffusion tends toward an equilibrium equalizing chemical potential, the equilibrium salt gradient is different from zero. Over a time interval τ, the heat transfer across the middle of the segment ΔQ is given by:

$$\Delta Q = \int_{M/2}^{M} C_p\Delta t\, dm \simeq \int_{M/2}^{M} C_p\Delta\frac{dt}{dm}(m - M/2)\, dm \simeq -\rho^2 C_p\tau k_t\frac{dt}{dm},$$

which yields an estimate for the temperature gradient perturbation:

$$\Delta\frac{dt}{dm} \simeq -8\frac{\rho^2\tau k_t}{M^2}\left(\frac{dt}{dm}\right). \tag{4}$$

Similarly, the salt flux perturbation is:

$$\Delta\frac{ds}{dm} \simeq -8\frac{\rho^2\tau k_s}{M^2}\left[\frac{ds}{dm} - \left(\frac{ds}{dm}\right)_{equil}\right],$$
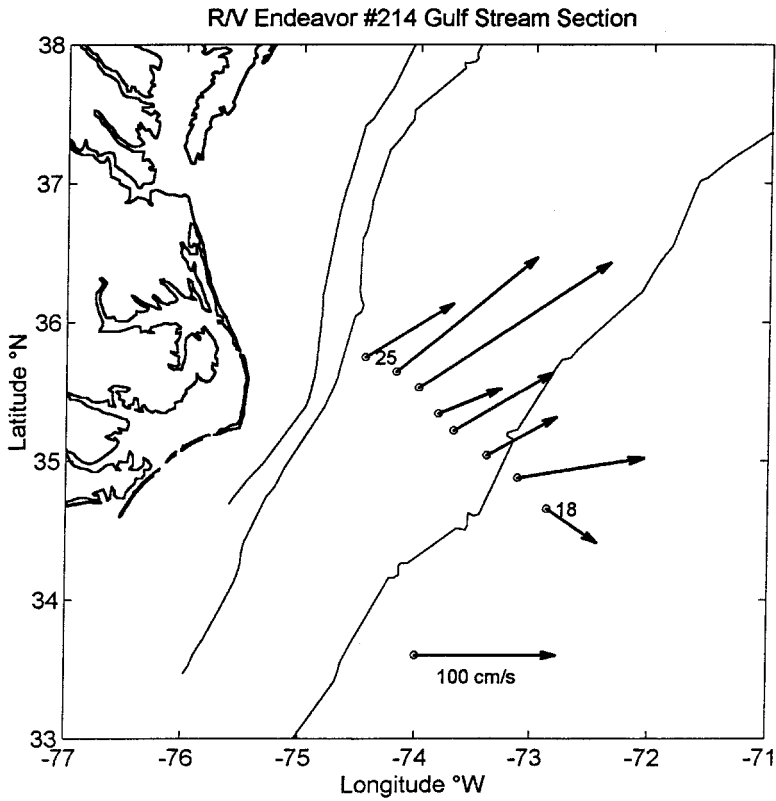
Figure 1. R/V *Endeavor* #214 *CTD* section across the Gulf Stream. Arrows show averaged velocities in the upper 1000 m (Pickart and Smethie, 1993).

so that the total change of *GPE* is:

$$\Delta \chi_{total} \simeq -\frac{4}{3} M \rho^2 \tau \left\{ k_t \frac{d}{dm} \left(p \frac{\partial \alpha}{\partial t} \right) \frac{dt}{dm} + k_s \frac{d}{dm} \left(p \frac{\partial \alpha}{\partial s} \right) \left[\frac{ds}{dm} - \left(\frac{ds}{dm} \right)_{equil} \right] \right\}.$$

The contribution from the salt diffusion is small $k_s \ll k_t$ so that the total *GPE* change is approximated by:

$$\Delta \chi_{total} \simeq -\frac{4}{3} M \rho^2 \tau \left[\frac{d}{dm} \left(p \frac{\partial \alpha}{\partial t} \right) \right] k_t \frac{dt}{dm}. \tag{5}$$

The temperature gradient *dt/dm* is generally positive so that potential instabilities will occur if $p(\partial \alpha / \partial t)$ decreases with depth and pressure.

Examples of the variation of $p(\partial \alpha / \partial t)$ versus pressure and potential temperature are taken from a CTD section (Fig. 1) across the Gulf Stream (Pickart and Smethie, 1993) and
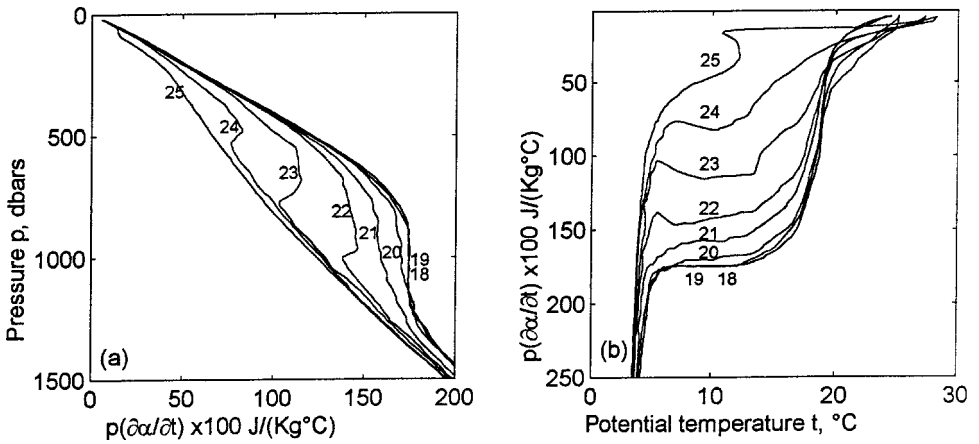
Figure 2. Plots of $p(\partial\alpha/\partial t)$ vs. pressure p (a), and potential temperature (b) for the *CTD* section shown in Figure 1.

shown in Figure 2. If $p(\partial\alpha/\partial t)$ is constant with pressure while the temperature is decreasing, the potential instability can be seen more dramatically by plotting against potential temperature (Fig. 2b), especially for the near surface thermocline at CTD #25.

A critical diffusive temperature gradient $(dt/dm)_{diff}$ occurs when:

$$\frac{d}{dm}\left(p\,\frac{\partial\alpha}{\partial t}\right) = \frac{\partial\alpha}{\partial t}\frac{dp}{dm} + p\left[\frac{\partial^2\alpha}{\partial t\partial p}\frac{dp}{dm} + \frac{\partial^2\alpha}{\partial t^2}\left.\frac{dt}{dm}\right|_{diff} + \frac{\partial^2\alpha}{\partial t\partial s}\frac{ds}{dm}\right] = 0.$$

Solving for $(dt/dm)_{diff}$ yields:

$$\left.\frac{dt}{dm}\right|_{diff} = \left[g\left(\frac{\partial\alpha}{\partial t} + p\frac{\partial^2\alpha}{\partial t\partial p}\right) - p\frac{\partial^2\alpha}{\partial t\partial s}\frac{ds}{dm}\right]\bigg/ p\frac{\partial^2\alpha}{\partial t^2} = \alpha\left.\frac{dt}{dz}\right|_{diff} = -g\left.\frac{dt}{dp}\right|_{diff}. \qquad (6)$$

Discussion and examples of diffusive and turbulent critical temperature gradients are given in Section 4.

3. Turbulent mixing

Turbulent mixing is simulated by an adiabatic vertical exchange of two elements of equal mass dm followed by mixing by diffusion with a surrounding water mass εdm where the ratio may vary over the range $0 \le \varepsilon \le \infty$. The contribution to *GPE* consists of three parts. The elements exchanged are equal in mass but different in volume, thus shifting the column between them. This shift produces a local change of *GPE* and an equal net change of enthalpy of the two elements. The exchanged elements have different compressibilities so that a net change in volume of the elements shifts the surrounding water relative to the gravitational field producing a global change of *GPE*. The internal energy of the two mass

elements is changed by an equal magnitude but of opposite sign. Mixing by diffusion with surrounding water after the exchange will not change enthalpy but, because of the volume change, will produce a global change of *GPE* and an equal but opposite change of the internal energy of the mixed mass elements.

The adiabatic exchange of mass elements produces a local *GPE* change, $\Delta\chi_{loc}$, by shifting the water column of thickness Δz and mass $\rho\Delta z$ vertically by the difference in thickness of the exchanged mass elements $(\alpha_2^f - \alpha_1^i)dm$, i.e.,

$$\Delta\chi_{loc} = \rho g\Delta z(\alpha_2^f - \alpha_1^i)dm.$$

The initial volume element at level 2, α_2^i, is shifted vertically downward to level 1 by Δz so that:

$$\alpha_2^f = \alpha_2^i - \left(\frac{\partial\alpha}{\partial z}\right)_a \Delta z + \cdots$$

Substituting and expanding by Taylor series yields:

$$\Delta\chi_{loc} = \rho g\Delta z\left[\alpha_2^i - \alpha_1^i - \left(\frac{\partial\alpha}{\partial z}\right)_a \Delta z\right]dm \simeq \rho g\left[\frac{d\alpha}{dz} - \left(\frac{\partial\alpha}{\partial z}\right)_a\right]\Delta z^2 dm \simeq 2dm\Delta z^2 E_{loc}, \tag{7}$$

where $E_{loc} = \frac{1}{2}N^2$ is the *GPE* change per unit mass and unit displacement and N is the Brunt-Väisälä frequency.

The external change $\Delta\chi_{ext}$ results from the different compressibilities of the exchanged elements shifting a mass $p_0/\rho g$ vertically by the volume change per unit area, i.e.,

$$\Delta\chi_{ext} = p_0(\alpha_2^f - \alpha_2^i + \alpha_1^f - \alpha_1^i)dm \simeq p_0 g\left[\frac{d\kappa}{dz} - \left(\frac{\partial\kappa}{\partial z}\right)_a\right]\Delta z^2 dm \simeq 2dm\Delta z^2 E_{ext}, \tag{8}$$

where $\kappa = -\frac{1}{\alpha}(\partial\alpha/\partial p)_a$ is adiabatic compressibility.

The exchanged mass element dm is mixed by diffusion with εdm of surrounding water at level 2. The change of volume on mixing, (see Appendix), is given by:

$$\Delta V_2 = (dm + \varepsilon dm)\alpha_{mix} - (dm\alpha_1^f + \varepsilon dm\alpha_2^i)$$

$$\simeq -\frac{1}{2}\frac{\varepsilon dm}{1+\varepsilon}\left[\frac{\partial^2\alpha}{\partial t^2}\Delta t^2 + 2\frac{\partial^2\alpha}{\partial t\partial s}\Delta t\Delta s + \frac{\partial^2\alpha}{\partial s^2}\Delta s^2\right]$$

and the contribution to *GPE* on mixing χ_{mix2} is given by

$$\Delta\chi_{mix2} = p_0\Delta V_2 \simeq -\frac{1}{2}\frac{\varepsilon dm}{1+\varepsilon}p_0\left[\frac{\partial^2\alpha}{\partial t^2}\Delta t^2 + 2\frac{\partial^2\alpha}{\partial t\partial s}\Delta t\Delta s + \frac{\partial^2\alpha}{\partial s^2}\Delta s^2\right] \tag{9}$$

where

$$\Delta t = t_2 - t_1 + \Gamma\Delta z = \theta_z \Delta z$$
$$\Delta s = s_2 - s_1 = s_z \Delta z.$$

A similar contribution $\Delta\chi_{mix1}$ occurs at level 1, so that

$$\Delta\chi_{mix} = \Delta\chi_{mix1} + \Delta\chi_{mix2} = -2dm\Delta z^2 \frac{\varepsilon}{1+\varepsilon} E_{mix}. \tag{10}$$

The total change of GPE per unit mass and unit displacement is, therefore:

$$E_{GPE} = E_{loc} + E_{ext} - \frac{\varepsilon}{1+\varepsilon} E_{mix} = \frac{1}{2}\left\{\rho g\left[\frac{d\left(\alpha - p_0\left(\frac{\partial\alpha}{\partial p}\right)_a\right)}{dz} - \left|\frac{\partial\left(\alpha - p_0\left(\frac{\partial\alpha}{\partial p}\right)_a\right)}{\partial z}\right|_a\right]\right.$$
$$\left. - \frac{\varepsilon}{1+\varepsilon} p_0\left(\frac{\partial^2\alpha}{\partial t^2}\theta_z^2 + \frac{\partial^2\alpha}{\partial t\partial s}\theta_z s_z + \frac{\partial^2\alpha}{\partial s^2}s_z^2\right)\right\}. \tag{11}$$

The limiting case for turbulent mixing is assumed to occur for diffusion with a large volume of surrounding water after the exchange, i.e., $\varepsilon \to \infty$. The critical turbulent gradient $(dt/dz)_{turb}$ occurs for $E_{GPE} = 0$.

4. Critical temperature gradients

The two types of perturbation described earlier are considered limiting cases for diffusive and turbulent mixing. The critical vertical temperature gradient for diffusive mixing is larger in magnitude than the turbulent critical gradient in regions where the salinity stratification is destabilizing. Salt content is transferred more rapidly by turbulent mixing than by diffusion alone. In regions of active mixing, the vertical gradients are expected to lie between these two limits. For vertical gradients below or above these limits, energy for mixing must come primarily from other sources such as velocity shear produced by tides or internal waves, for example. Stable maximum vertical temperature gradients should not exceed the diffusive limit according to this hypothesis if mixing is weak. Several examples are presented to support this conclusion.

A striking example of a limiting diffusive gradient is exhibited by the North Atlantic subtropical thermocline. The gradient is assumed to be strengthened by the downwelling waters driven by convergent Ekman flow in the surface layers and a deep upwelling driven by convergent deep water flow (Robinson and Stommel, 1959). The vertical gradient in the thermocline is assumed to increase until limited by mixing processes (Munk, 1966). The observed gradient reaches the diffusive limit suggesting that the turbulence within the thermocline is not the dominant energy source. An example is presented from a CTD section (Fig. 1) across the Gulf Stream. The data are taken from one of a series of sections carried out by Pickart and Smethie (1993). As can be seen from Figure 2a,b, plots of $p(\partial\alpha/\partial t)$ vs pressure and potential temperature show decreasing values where the vertical

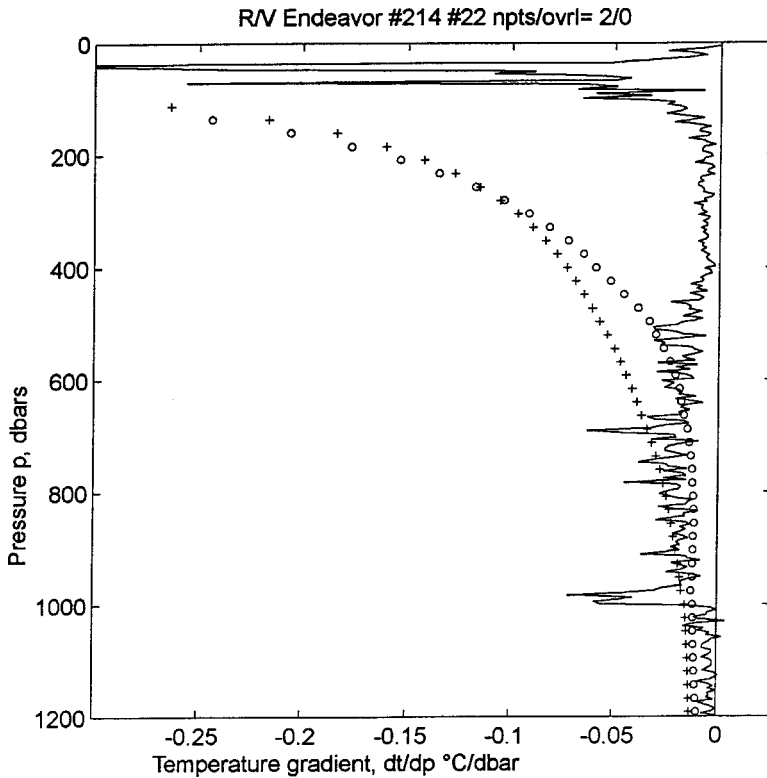Figure 3. Vertical temperature gradients for R/V *Endeavor* #214 *CTD* #22. (+) diffusive critical
gradient; (○) turbulent critical gradient; (—) measured vertical gradient.

temperature gradients within the thermocline exceed the diffusive limit. These occur along
the high-velocity inshore layer of the Gulf Stream where vertical shear is high. On the
ocean side, the vertical gradients are at the diffusive limit. The vertical structure of the
diffusive and turbulent critical gradients at Station #22 is shown in Figure 3. Throughout
the main thermocline from 500 to 1000 dbars, the vertical temperature gradient fluctuates
between the turbulent and diffusive limits with an average close to the turbulent limit. The
conclusion is that the vertical mixing reduces as much *GPE* globally as is increased locally
throughout the entire thickness of the thermocline. Thus, the volume change represents a
significant secondary source of energy for the velocity field. The vertical temperature
gradients gradually relax downstream to the diffusive limit. At a section along 68W shown
in Figure 4a, b (Hall and Fofonoff, 1993), the average vertical temperature gradient of the
inshore layer in the main thermocline does not exceed the diffusive limit. Although the
average thermocline gradients are at the diffusive limit, small-scale structures can be seen
that fluctuate about this limit (Fig. 5). At gradients below the critical diffusive limit, the
contraction on mixing is not the dominant energy source and presumably plays a lesser role
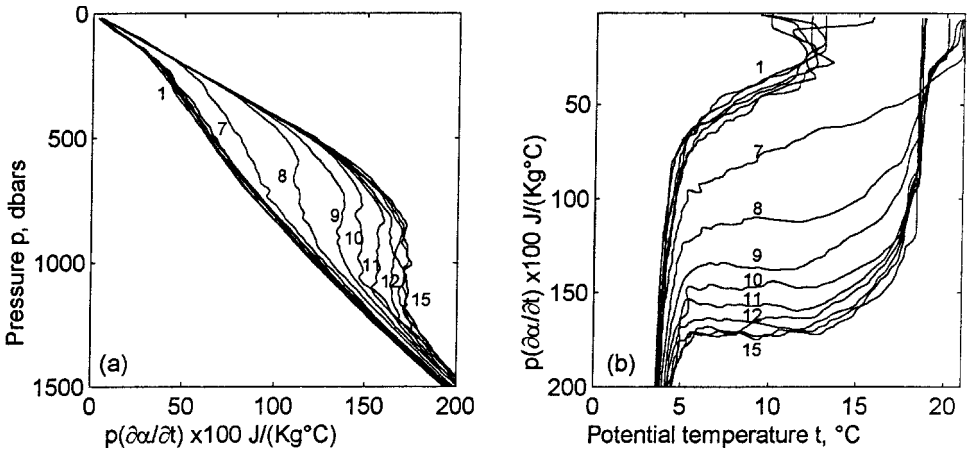in mixing processes affecting the vertical gradients.

Figure 4. Plots of $p(\partial\alpha/\partial t)$ vs pressure p (a), and potential temperature (b) for R/V *Endeavor* #175 *CTD* section along 68W (Hall and Fofonoff, 1993).
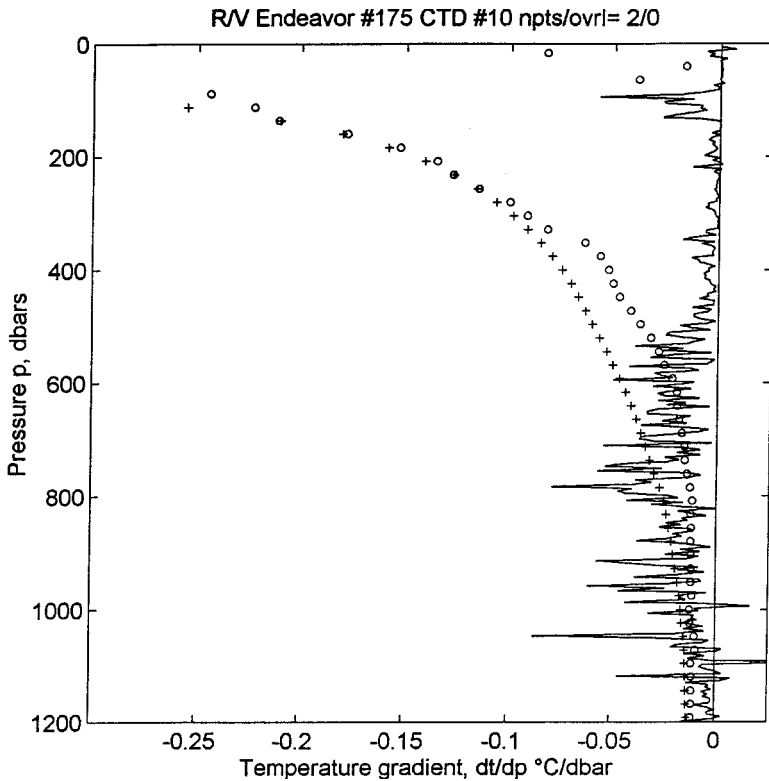

Figure 5. Vertical temperature gradients for R/V *Endeavor* #175 *CTD* #10. (+) diffusive critical gradient; (○) turbulent critical gradient; (—) measured vertical gradient.
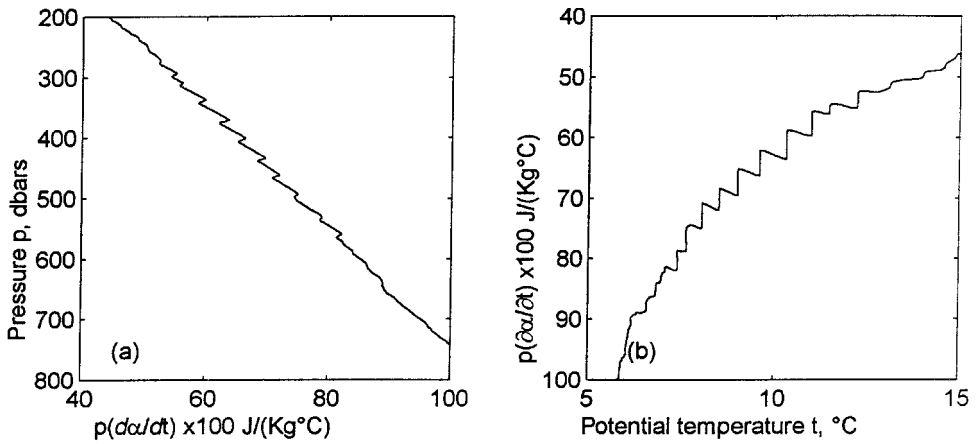
Figure 6. Plots of $p(\partial\alpha/\partial t)$ vs pressure p (a), and potential temperature (b) for R/V *Knorr* #118 $C-$ *SALT HRP* #27 showing thermohaline step structure (Schmitt *et al.,* 1987).

A turbulent limit for staircase structures is illustrated in Figure 6a, b. A High Resolution Profiler (*HRP*) Station #27, taken during the Caribbean-Sheets and Layer Transects, $C-$ *SALT,* project (Schmitt *et al.,* 1987), revealed active salt finger layers at depths of 300 to 500 m. The vertical temperature gradients at the interfaces exceeded the critical turbulent gradients by an order of magnitude. However, a vertical average over the layers yields mean gradients at the turbulent gradient limit (Fig. 7a, b). The interpretation is that the staircase structure derives significant energy from the *GPE* conversion. A possible interpretation is that the total step thickness Δz and the interfacial thickness Δz_i adjust to maintain turbulence in the layer. If the steps in temperature, salinity and velocity are given by Δt, Δs, Δu, the average Richardson number R_{av} is:

$$R_{av} = N^2/(du/dz)^2 = \rho g \left| \frac{\partial\alpha}{\partial t}\frac{\Delta t}{\Delta z} + \frac{\partial\alpha}{\partial s}\frac{\Delta s}{\Delta z} \right| \Big/ \left(\frac{\Delta u}{\Delta z}\right)^2, \qquad (12)$$

where $\Delta t/\Delta z$ is equal to the critical turbulent gradient. For the interfacial layer, the Richardson number is:

$$R_i = N^2/(du/dz)^2 = \rho g \left| \frac{\partial\alpha}{\partial t}\frac{\Delta t}{\Delta z_i} + \frac{\partial\alpha}{\partial s}\frac{\Delta s}{\Delta z_i} \right| \Big/ \left(\frac{\Delta u}{\Delta z_i}\right)^2,$$

then:

$$R_i/R_{av} = \Delta z_i/\Delta z.$$

For a critical Richardson number at the interfaces, $R_i \leq \frac{1}{4}$, the ratio becomes $\Delta z_i/\Delta z \leq 1/(4R_{av})$, determined by the average density and velocity gradient.
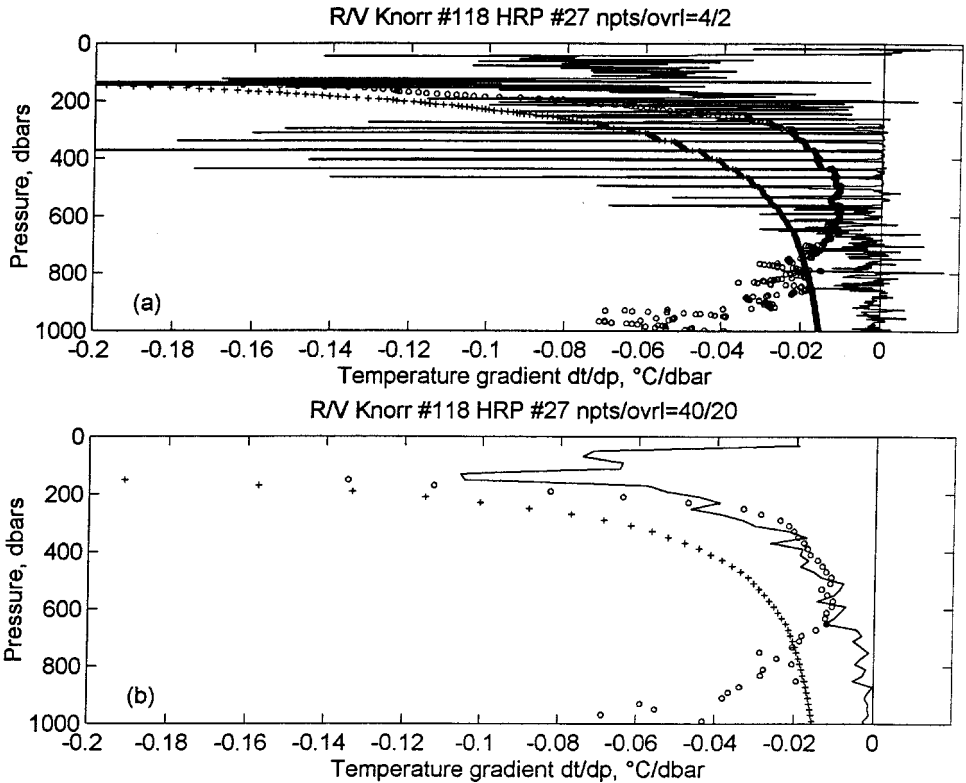
Figure 7. Vertical temperature gradients for R/V *Knorr* #118 *HRP* #27. The measured gradients are averaged over *npts* successive data points overlapped by *ovrl* for successive pressure intervals. (+) diffusive critical gradient; (○) turbulent critical gradient; (—) measured vertical gradient.

5. Kinetic energy

The momentum equations yield the following equation for changes of kinetic energy $k_e = \frac{1}{2} u_i u_i$:

$$\rho \frac{\partial k_e}{\partial t} + \rho u_j \frac{\partial k_e}{\partial x_j} = -u_j \frac{\partial p}{\partial x_j} - \rho u_j \frac{\partial \phi}{\partial x_j} + \text{viscous terms.} \qquad (13)$$

The source terms for kinetic energy are the enthalpy flux or pressure work term, $-u_j(\partial p/\partial x_j)$, and the conversion to and from *GPE*, $-\rho u_j(\partial \phi/\partial x_j)$. The viscous terms also contribute depending on the velocity gradients. The primary conversion for displacements is between enthalpy and *GPE*, representing hydrostatic balance. Conversion of enthalpy to and from kinetic energy occurs for flow along a geopotential surface if pressure changes occur along a streamline. Similarly, kinetic energy is changed for flow along a pressure surface if the gravitational potential changes along a streamline. Changes in the volume of a water mass by diffusion and mixing will shift mass and pressure surfaces relative to the gravitational field and contribute to the kinetic energy changes.

A similar interpretation can be made from the energy conservation equation:

$$\rho \frac{\partial (k_e + h)}{\partial t} + \rho u_j \frac{(k_e + h)}{\partial x_j} = \frac{\partial p}{\partial t} - \rho u_j \frac{\partial \phi}{\partial x_j} + \text{viscous and diffusive terms.} \quad (14)$$

Volume changes by mixing produce global shifts of mass that do not change enthalpy requiring, therefore, a conversion of *GPE* to kinetic energy. This can be seen more easily for a steady state, $\partial p/\partial t = 0$, where the contribution from mass shifts is between kinetic energy and *GPE*.

Using the same adiabatic exchange of two elements of mass dm with velocities u_1, u_2 and mixing with εdm of surrounding water, the change of kinetic energy at level 2 is:

$$\Delta k_{e2} = \frac{1}{2} (dm + \varepsilon dm)(u_2^f)^2 - \frac{1}{2} (dmu_1^2 + \varepsilon dmu_2^2).$$

Assuming that momentum is conserved, the final velocity u_2^f will be:

$$u_2^f = (u_1 + \varepsilon u_2)/(1 + \varepsilon).$$

Similarly, at level 1:

$$u_1^f = (\varepsilon u_1 + u_2)/(1 + \varepsilon)$$

$$\Delta k_{e1} = \frac{1}{2} (dm + \varepsilon dm)(u_2^f)^2 - \frac{1}{2} (\varepsilon dmu_1^2 + dmu_2^2)$$

so that the total change of kinetic energy is:

$$(\Delta k_{e2} + \Delta k_{e1})/(2dm\Delta z^2) = -\frac{1}{2} \frac{\varepsilon}{1 + \varepsilon} \left|\frac{du}{dz}\right|^2 = -\frac{\varepsilon}{1 + \varepsilon} E_{k_e}. \quad (15)$$

The exchange and mix perturbation produces a total change of energy per unit mass and unit length, E_{total}, of:

$$E_{total} = E_{local} + E_{ext} - \frac{\varepsilon}{1 + \varepsilon} (E_{k_e} + E_{mix}). \quad (16)$$

Of these, E_{mix} can be considered an energy source term for kinetic energy and E_{k_e} a source term for local mixing. The contribution of these two terms depends on the mass ratio ε of mixing with surrounding waters.

The hypothesis proposed here is that long-term stability requires $E_{total} > 0$. If the global changes of *GPE* offset the local changes, the kinetic energy level will be maintained or increased. Thus, structures that yield a net decrease of total *GPE* for local perturbations will have a more rapid decay rate toward a stable state where any perturbation will increase the total *GPE*. Thus, the relative stability of an ocean structure can be examined by comparing the critical gradients with measured temperature gradients.

A necessary condition for instability by vertical velocity shear in stratified flow is for the classical Richardson number $Ri = N^2/(du/dz)^2 = E_{loc}/E_{k_e} \leq 1$ (Richardson, 1920), and a sufficient condition for parallel shear flow for $Ri \leq \frac{1}{4}$ (Goldstein, 1931; Taylor, 1931). This range of Ri can be expressed as:

$$E_{loc} \leq E_{k_e} \leq 4E_{loc},$$

or:

$$N^2 \leq \left|\frac{du}{dz}\right|^2 \leq 4N^2.$$

The perturbations described above yield an excess of energy for mixing when:

$$\frac{\varepsilon}{1 + \varepsilon}(E_{k_e} + E_{mix}) \geq (E_{loc} + E_{ext}).$$

The relative magnitudes of the energy sources and sinks can be described by a modified Richardson number Ri^* defined as:

$$Ri^* = \frac{\varepsilon}{1 + \varepsilon} = \left[\frac{E_{local} + E_{ext}}{E_{k_e} + E_{mix}}\right]. \tag{17}$$

For values $0 \leq Ri^* \leq 1$, the total energy change, E_{total}, is negative and the mixing is presumably energized by the velocity shear and the nonlinear contributions. For complete mixing $\varepsilon \to \infty$, $Ri^* \leq 1.0$. For partial mixing $\varepsilon \simeq \frac{1}{3}$, Ri^* has the classical value of $\frac{1}{4}$. Comparisons of Ri^* and the classical Ri are shown for stations in the North Atlantic (Fig. 8) and the Brazil basin (Fig. 9).

Both E_{loc} and E_{ext} are linear functions of the vertical gradients of temperature and salinity, while E_{mix} and E_{k_e} are quadratic functions. Thus, both E_{mix} and E_{k_e} are very sensitive to the averaging used to estimate gradients from measurements using *CTD*s and high-resolution profilers *HRP*s. To examine the dependence on averaging, the vertical gradients were estimated by fitting a linear and a cubic least-square polynomial in pressure to the temperature, salinity and velocity measurements. An interval of n cycles ranging from 4 to 40 at 0.5 decibar intervals was used to calculate a sequence of least-square fits. Each variable was averaged over m intervals with the fitting interval advanced by *novl* for each fit, where *novl* is the number of overlay cycles with the previous interval. Examples are shown in Figures 8 and 9. The highest resolution, $n = 4$, yields values for $E_{k_e} + E_{mix}$ near or above the classical limit, $Ri^* = \frac{1}{4}$. At the highest smoothing, $n = 40$, the values are closer to $Ri^* = 1$. Addition of the nonlinear *GPE* conversions to the kinetic energy term results in a closer agreement with these limits. A possible interpretation is that the classical Richardson number criterion for shear instabilities applies at the smallest scales, while the modified Richardson number is effective at larger scales. As measurement noise would also increase the average quadratic mean of the gradient at the highest resolution, the
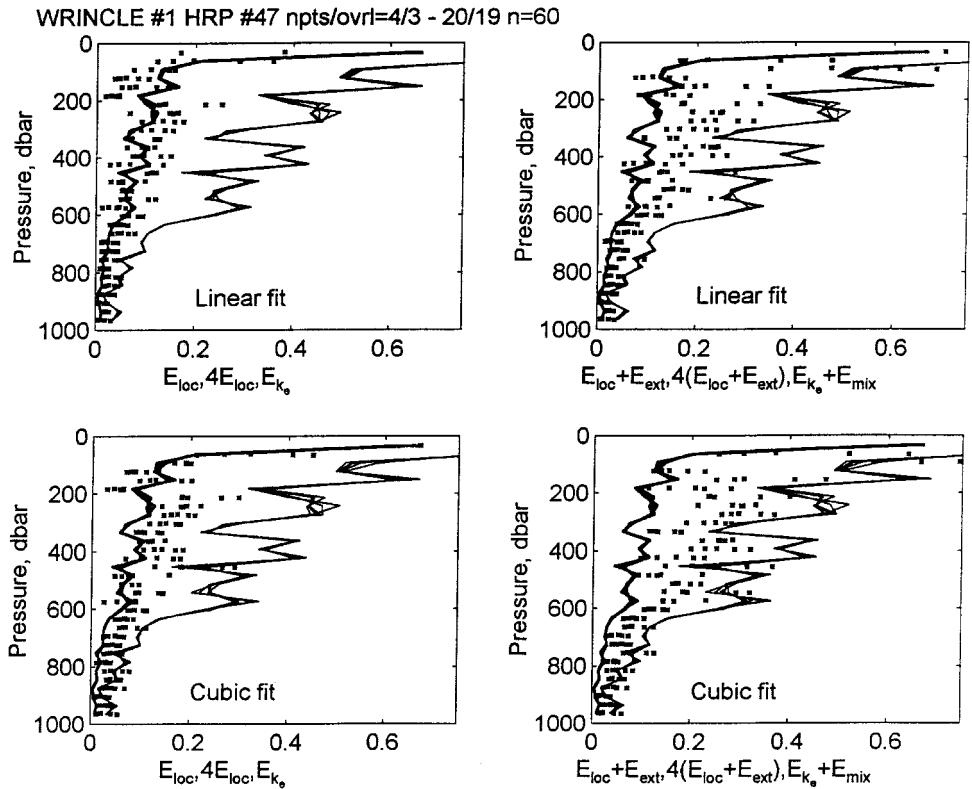
WRINCLE #1 HRP #47 npts/ovrl=4/3 - 20/19 n=60

Figure 8. R/V *Oceanus* #218 *HRP* #47. Vertical distribution of the linear energy parameters, E_{loc}, E_{ext}, and the second-order parameters, E_{mix}, E_{k_e}, plotted in units of 10^{-4} sec^{-2}. The linear parameters, shown by solid lines, are not sensitive to vertical averaging.

interpretation must be viewed with some caution. However, the fact that the magnitude of the local and global energy sources, $E_{k_e} + E_{mix}$, falls within the narrow limits set by $\frac{1}{4} \leq Ri^* \leq 1$ is strong evidence for the role of the nonlinear contributions to energy conversions in limiting vertical gradients in the oceans.

6. Conclusions

The strong dependence of the thermal expansion of seawater on temperature and pressure places constraints on the structure of the temperature, salinity and density fields in the ocean. Vertical temperature gradients sharper than the critical magnitudes described above, will allow more energy to be released to the column above than is consumed by local perturbations. By analogy, a block of ice placed on a sloping surface will slide and accelerate until dissipation at the interface reaches the rate of decrease of *GPE* of the sliding block. The Gulf Stream is slippery in this sense. Downstream from Cape Hatteras, a net release of *GPE* for vertical mixing occurs along the high-velocity inshore layer. The
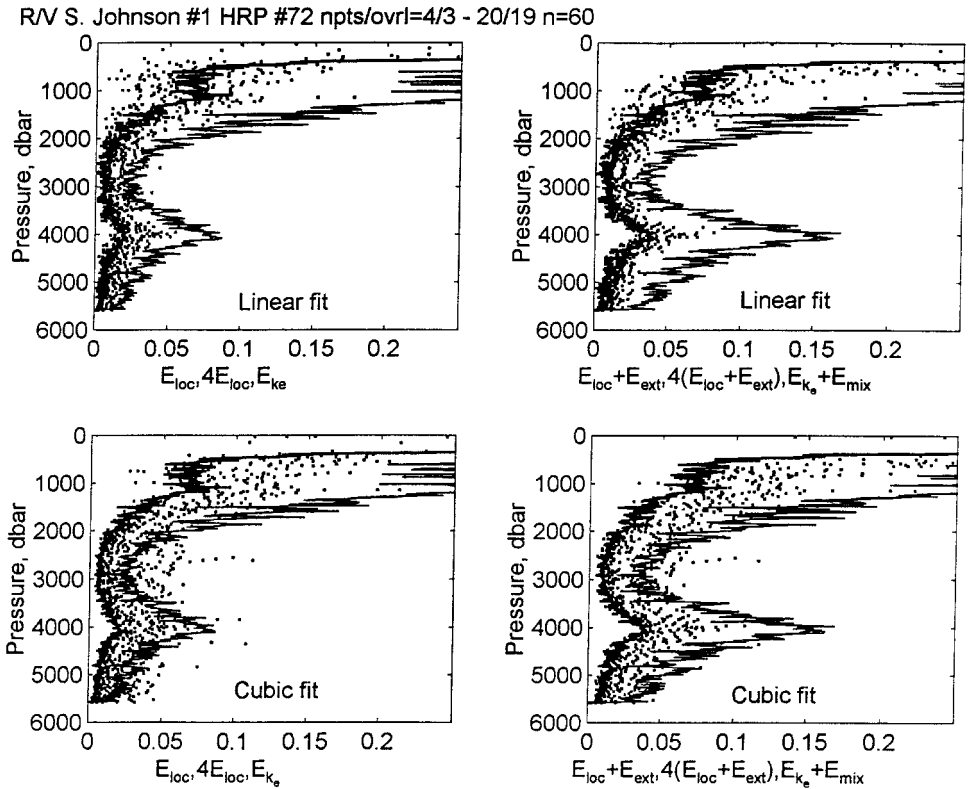
R/V S. Johnson #1 HRP #72 npts/ovrl=4/3 - 20/19 n=60

Figure 9. R/V S. *Johnson* #1 *HRP* #72. Vertical distribution of the linear energy parameters, E_{loc}, E_{ext}, and the second-order parameters, E_{k_e}, E_{mix}, plotted in units of $10^{-4} \sec^{-2}$.

gradients weaken downstream to the turbulent limit and finally to the diffusive limit that is characteristic of the thermocline gradient throughout the North Atlantic basin.

A very different case can be seen for the staircase structure described by the $C - SALT$ data. Here, the temperature gradients at the interface layers strongly exceed both turbulent and diffusive critical magnitudes. However, the vertical average of the gradient over the staircase scale closely parallels the turbulent limiting gradient. Although the interpretation is not entirely clear, the effect of the nonlinear energy release mechanism must play an important role in setting the scales of the staircase structure.

Preliminary examination of *CTD* and *HRP* stations in other ocean basins indicates that the critical gradients play a role in surface mixed-layer dynamics, in equatorial undercurrents as well as in structures such as warm/cold rings and meddies. Further studies are needed.

APPENDIX

The change of a thermodynamic function, λ, resulting from mixing of two mass elements of seawater, m_1, m_2, at constant pressure p, can be estimated by expanding the function in a Taylor series in terms of the conserved properties, salinity s and enthalpy h. The final values are denoted by a superscript f.

Conservation of mass is expressed by:

$$\Delta m^f = m^f - (m_1 + m_2) = 0.$$

Total internal energy $m^f e^f$, changed by pressure work, is given by:

$$m^f \Delta e^f = m_1 \Delta e_1 + m_2 \Delta e_2 = -m_1 p \Delta \alpha_1 - m_2 p \Delta \alpha_2,$$

which is equivalent to conservation of enthalpy:

$$m_1 (\Delta e_1 + p \Delta \alpha_1) + m_2 (\Delta e_2 + p \Delta \alpha_2) = m_1 \Delta h_1 + m_2 \Delta h_2 = m^f \Delta h^f = 0.$$

Salinity, interpreted as a mass ratio, is conserved:

$$m^f \Delta s^f = m^f s^f - (m_1 s_1 + m_2 s_2) = m_1 \Delta s_1 + m_2 \Delta s_2 = 0.$$

Similarly, an arbitrary thermodynamic function, λ, changes by:

$$m^f \Delta \lambda^f = m_1 (\Delta \lambda^f - \Delta \lambda_1) + m_2 (\Delta \lambda^f - \Delta \lambda_2) = m_1 \Delta \lambda_1 + m_2 \Delta \lambda_2.$$

Expanding $\Delta \lambda_1$, $\Delta \lambda_2$ in terms of the changes of enthalpy, Δh_1, Δh_2 and salinity, Δs_1, Δs_2 yields:

$$\Delta \lambda_1 = \frac{\partial \lambda}{\partial h} \Delta h_1 + \frac{\partial \lambda}{\partial s} \Delta s_1 - \frac{1}{2} \left| \frac{\partial^2 \lambda}{\partial h^2} (\Delta h_1)^2 + 2 \frac{\partial^2 \lambda}{\partial h \partial s} \Delta h_1 \Delta s_1 + \frac{\partial^2 \lambda}{\partial s^2} (\Delta s_1)^2 \right) + \cdots$$

$$\Delta \lambda_2 = \frac{\partial \lambda}{\partial h} \Delta h_2 + \frac{\partial \lambda}{\partial s} \Delta s_2 - \frac{1}{2} \left| \frac{\partial^2 \lambda}{\partial h^2} (\Delta h_2)^2 + 2 \frac{\partial^2 \lambda}{\partial h \partial s} \Delta h_2 \Delta s + \frac{\partial^2 \lambda}{\partial s^2} (\Delta s_2)^2 \right) + \cdots$$

The first-order terms drop out on substituting the Taylor expansions and applying the conservation equations leaving only the second-order terms for changes of λ:

$$m^f \Delta \lambda^f = -\frac{1}{2} \left[\frac{\partial^2 \lambda}{\partial h^2} (m_1 (\Delta h_1)^2 + m_2 (\Delta h_2)^2) + \frac{\partial^2 \lambda}{\partial h \partial s} (m_1 \Delta h_1 \Delta s_1 + m_2 \Delta h_2 \Delta s_2) \right.$$

$$\left. + \frac{\partial^2 \lambda}{\partial s^2} (m_1 (\Delta s_1)^2 + m_2 (\Delta s_2)^2) \right] + \cdots$$

Since,

$$m_1(\Delta h_1)^2 + m_2(\Delta h_2)^2 = \frac{m_1 m_2}{m_1 + m_2}(\Delta(h_1 - h_2))^2$$

$$m_1 \Delta h_1 \Delta s_1 + m_2 \Delta h_2 \Delta s_2 = \frac{m_1 m_2}{m_1 + m_2}(\Delta(h_1 - h_2)\Delta(s_1 - s_2))$$

$$m_1(\Delta s_1)^2 + m_2(\Delta s_2)^2 = \frac{m_1 m_2}{m_1 + m_2}(\Delta(s_1 - s_2))^2,$$

the final expression for the change is:

$$m^f \Delta \lambda^f = -\frac{1}{2}\frac{m_1 m_2}{m_1 + m_2}\left[\frac{\partial^2 \lambda}{\partial h^2}(\Delta h)^2 + 2\frac{\partial^2 \lambda}{\partial h \partial s}\Delta h \Delta s + \frac{\partial^2 \lambda}{\partial s^2}(\Delta s)^2\right] + \cdots$$

Expressing enthalpy derivatives in terms of temperature and salinity yields:

$$m^f \Delta \lambda^f = -\frac{1}{2}\frac{m_1 m_2}{m_1 + m_2}\left[\frac{\partial^2 \lambda}{\partial t^2}(\Delta t)^2 + 2\frac{\partial^2 \lambda}{\partial t \partial s}\Delta t \Delta s + \frac{\partial^2 \lambda}{\partial s^2}(\Delta s)^2\right.$$
$$\left. -\frac{1}{C_p}\frac{\partial \lambda}{\partial t}\left|\frac{\partial^2 h}{\partial t^2}(\Delta t)^2 + 2\frac{\partial^2 h}{\partial t \partial s}\Delta t \Delta s + \frac{\partial^2 h}{\partial s^2}(\Delta s)^2\right|\right] + \cdots$$

The change of volume by mixing, substituting α for λ, is estimated by:

$$m^f \Delta \alpha^f \simeq -\frac{1}{2}\frac{m_1 m_2}{m_1 + m_2}\left[\frac{\partial^2 \alpha}{\partial t^2}(\Delta t)^2 + 2\frac{\partial^2 \alpha}{\partial t \partial s}\Delta t \Delta s + \frac{\partial^2 \alpha}{\partial s^2}(\Delta s)^2\right]$$

since the variation of specific heat, $C_p = \partial h/\partial t$, with temperature and salinity does not contribute significantly to the volume change.

REFERENCES

Charney, J. G. and A. Eliassen. 1964. On the growth of the hurricane depression. J. Atmos. Sci., *21,* 68–75.

Eckel, O. 1949. Uber die Mischungsarbeit von stabil geschichteten Wassermassen. Arch. Met., Wien, Ser. A, *1,* 264–269.

Feistel, R. and E. Hagen. 1995. On the *GIBBS* thermodynamic potential of seawater. Prog. Oceanogr., *36,* 249–327.

Fofonoff, N. P. 1961. Energy transformations in the sea. (Unpublished) Manuscript Report Series 109, Fish. Res. Bd., Canada, 82 pp.

—— 1995. Dynamical effects of cabbeling on thermocline structure. (in Russian, English abstract). Okeanologia, *35,* 824–832.

Gill, A. E. 1973. Circulation and bottom water production in the Weddell Sea. Deep-Sea Res., *20,* 111–140.

Goldstein, S. 1931. On the stability of superimposed streams of fluid of different densities. Proc. Roy. Soc., A *132,* 524–548.

Hall, M. M. and N. P. Fofonoff. 1993. Downstream development of the Gulf Stream from 68 to 55 W. J. Phys. Oceanogr., *23,* 225–249.

Munk, W. H. 1966. Abyssal recipes. Deep-Sea Res., *13,* 707–730.

Pickart, R. S. and W. M. Smethie. 1993. How does the deep Western Boundary Current cross the Gulf Stream? J. Phys. Oceanogr., *23,* 2602–2616.

Richardson, L. F. 1920. The supply of energy from and to atmospheric eddies. Proc. Roy. Soc. London, A *97,* 354–373.

Robinson, A. R. and H. Stommel. 1959. The oceanic thermocline and the associated thermohaline circulation. Tellus, *3,* 295–308.

Schmitt, R. W., H. Perkins, J. D. Boyd and M. C. Stalcup. 1987. *C-SALT:* An investigation of the thermohaline staircase in the western tropical North Atlantic. Deep-Sea Res., *34,* 1655–1665.

Taylor, G. I. 1931. Effect of variation of density on superimposed streams of fluid. Proc. Roy. Soc. London, A *132,* 499–523.

Witte, E. 1902. Zur Theorie der Stromkabbelungen. Gaea, Koln, *38,* 484–487.